



Effect of molecular desorption on the electronic properties of self-assembled polarizable molecular monolayers



Gunuk Wang^{a,b}, Hyunhak Jeong^c, Jamin Ku^b, Seok-In Na^d, Hungu Kang^e, Eisuke Ito^f, Yun Hee Jang^b, Jaegeun Noh^{e,*}, Takhee Lee^{c,*}

^a Department of Chemistry and the Smalley Institute for Nanoscale Science and Technology, Rice University, Houston, TX 77005, USA

^b School of Materials Science and Engineering, Gwangju Institute of Science and Technology, Gwangju 500-712, Republic of Korea

^c Department of Physics and Astronomy, Seoul National University, Seoul 151-747, Republic of Korea

^d School of Flexible and Printable Electronics, Chonbuk National University, Jeonju-si, Jeollabuk-do 561-756, Republic of Korea

^e Department of Chemistry, Hanyang University, Seoul 133-791, Republic of Korea

^f Flucto-Order Functions Research Team, RIKEN-HYU Collaboration Center, RIKEN, 2-1 Hirosawa, Wako, Saitama 351-0198, Japan

ARTICLE INFO

Article history:

Received 12 November 2013

Accepted 21 December 2013

Available online 27 December 2013

Keywords:

Self-assembled monolayer

Work function

Dipole moment

Thermal desorption

ABSTRACT

We investigated the interfacial electronic properties of self-assembled monolayers (SAM)-modified Au metal surface at elevated temperatures. We observed that the work functions of the Au metal surfaces modified with SAMs changed differently under elevated-temperature conditions based on the type of SAMs categorized by three different features based on chemical anchoring group, molecular backbone structure, and the direction of the dipole moment. The temperature-dependent work function of the SAM-modified Au metal could be explained in terms of the molecular binding energy and the thermal stability of the SAMs, which were investigated with thermal desorption spectroscopic measurements and were explained with molecular modeling. Our study will aid in understanding the electronic properties at the interface between SAMs and metals in organic electronic devices if an annealing treatment is applied.

© 2013 Elsevier Inc. All rights reserved.

1. Introduction

The use of self-assembled monolayers (SAM) of polarizable molecules has been recognized to be a convenient and useful chemical approach to enable the tuning of the electrical properties of organic-based devices [1–12]. In particular, a dipolar molecular layer on an electrode surface can control the two important electronic properties: the work function [2,4–9,11,12] and the injection barrier height [1,3–5,7–10] (which is the difference between the Fermi level of the electrode and the molecular orbital level) of the subsequently deposited organic active material. These two parameters, which depend on the dipole moment at the SAM/electrode interface, have been considered to be the main factors to be adjusted for efficient charge injection properties in organic electronic devices in various applications. For this reason, a considerable number of studies have investigated the influence of SAMs on the electronic properties of the metal surface and organic devices [1,3–5,7–10]. In addition, in organic electronic devices, the effect of thermal annealing on the properties of the interface between the SAM and the electrode surface is an interesting subject because annealing treatments of organic-based devices with SAMs are often employed to enhance the morphological and

interfacial electronic properties of the organic materials in the devices [5,13–15]. In particular, annealing can change the work function of a SAM-modified metal [5,16,17], that leads to change the electrical properties of organic electronic device. Therefore, it is important to understand the influence of the dipole moments for various types of SAM on the electronic properties of the metal surface at different temperatures for organic device application.

In this study, we investigated the influence of molecular desorption on the work function of SAM-modified Au metal surfaces under different temperature conditions with a Kelvin probe technique and compared the experimental results with those of theoretical calculations derived from the Helmholtz equation. We developed a comprehensive explanation for the values of the temperature-dependent work function of SAM-modified Au metal based on the molecular binding energy and the thermal stability of the SAM. These properties were also investigated with thermal desorption spectroscopic (TDS) measurements and molecular modeling.

2. Experimental

2.1. Preparation of the metal substrate

To prepare the metal substrate, a p-type (100) Si wafer (1 cm × 1 cm) covered with thermally grown, 300 nm thick SiO₂ was cleaned with a detergent and was ultrasonicated in acetone,

* Corresponding authors.

E-mail addresses: jgnoh@hanyang.ac.kr (J. Noh), tlee@snu.ac.kr (T. Lee).

methanol, and DI (deionized) water for ~ 10 min each. Then, the substrates were treated with UV (ultraviolet)/ozone to remove the remaining organic residues. Next, Ti (5 nm) and Au (100 nm) (99.999%) were deposited on the substrates with an electron beam evaporator under a pressure of $\sim 10^{-7}$ Torr at a low deposition rate of 0.1–0.2 Å/s. The average root-mean-square (RMS) roughness for the Au/Ti substrate was found to be ~ 0.8 Å by atomic force microscopy (AFM, Park Systems XE-100) for scan sizes of $2 \mu\text{m} \times 2 \mu\text{m}$ (not shown here).

2.2. SAM preparation

Three molecular species ((i) 2-naphthalenethiol (denoted Naph-S), (ii) 2-naphthyl isocyanide (Naph-NC), and (iii) 1H,1H,2H,2H-perfluorodecanethiol (Perfluoro-C10-S)) were self-assembled on the Au surface from molecular solutions in anhydrous ethanol. To form SAM of these molecules on the Au surface, we used 3 mM molecular solutions and an incubation time of at least two days in a nitrogen-filled glove box with an oxygen level of less than ~ 10 ppm to avoid potential oxidation problems. Before the Kelvin probe measurement, the SAM-modified Au substrate was rinsed with anhydrous ethanol and was dried under flowing N_2 . All molecular species in this study were purchased from the Aldrich Chem. Co.

2.3. Kelvin probe measurement

The work function of each SAM-modified Au sample was detected with a Kelvin probe (KP 6500 Digital Kelvin probe, McAllister Technical Services, Co.). To investigate the work function of the samples at elevated temperatures, the samples were annealed on a calibrated hotplate in a glove box for at least 10 min at different temperatures (300, 323, 343, 363 and 383 K). After cooling to room temperature, the samples were rinsed again with anhydrous ethanol and were dried under flowing N_2 to remove the residual desorbed molecules on the substrate. Then, the work function of the samples was measured with the Kelvin probe in the glove box. The contact potential difference was calibrated to highly ordered pyrolytic graphite (HOPG) at 4.58 ± 0.03 eV. The work function of the deposited Au/Ti metal on the SiO_2/Si substrate was found to be 4.94 ± 0.06 eV.

2.4. Thermal desorption spectroscopy measurement

To examine and compare the thermal desorption behavior and stability of the SAMs on the Au surfaces, thermal desorption spectroscopy (TDS) measurements (WA-1000S system, ESCO, Ltd.) were performed with a quadrupole mass spectrometer (QMG422; Balzers). The heating rate was approximately 1 K/s, and the surface temperature was measured with a chromel–alumel thermocouple in contact with the SAM/Au samples. The vacuum pressure in the chamber was less than 10^{-10} Torr. The desorption fragments for each SAM sample were detected as a function of surface temperature.

2.5. Molecular modeling

The potential drop ($\Delta\Phi$) of the SAM-modified Au metal substrates with various molecular species can theoretically be extracted from the Helmholtz equation (Eq. (1)) [4,18]. The dipole moments (μ in Table 1) of the molecular species (Naph-S, Naph-NC, and Perfluoro-C10-S) used in the equation were calculated for geometries optimized in the gas phase with density functional theory (DFT) at the B3LYP/6-311++G** level of theory and implemented in Jaguar v6.5. And the binding energies of the molecules adsorbed on the Au(111) surface were estimated with a classical

molecular mechanics calculation based on the final geometries, which were optimized with the conjugate gradient method for the universal force field (UFF) [19,20] (see Table 2).

3. Results and discussion

We used three types of molecules (Fig. 1) to study the influence of the density and magnitude of the dipole moment on the SAM-modified metal surfaces. The molecular systems investigated in this study can be categorized by three different features based on chemical anchoring group ($-\text{S}$ or $-\text{NC}$), molecular backbone structure (naphthalene or perfluorodecane), and the direction of the dipole moment (from metal to molecule or vice versa). The direction of the molecular dipole moment is defined by the direction from the negative charge (δ^-) to the positive charge (δ^+) for molecules whose charge distribution has non-uniform polarity [8]. In our molecular systems, the direction of the dipole moment for Naph-S and Naph-NC is oriented from Au metal (δ^-) to the molecular material (δ^+). In contrast, the direction of the dipole moment for Perfluoro-C10-S is oriented from the molecular material (δ^-) to the Au metal (δ^+) because of the relatively high electronegativity of the fluorine atoms [4]. The direction and magnitude of the dipole moments of the molecular systems were calculated with DFT for unbound and isolated (gas phase) molecules (see Table 1).

In the energy level diagrams for the SAM/Au interface shown in Fig. 2, the directionality of the dipole moment determines the sign of the interfacial potential drop ($\Delta\Phi$) with respect to the Fermi level of the Au reference metal. Therefore, the direction of the dipole moment can change the work function (Φ_w) of the SAM-modified Au metal. For example, Naph-S and Naph-NC molecules, with dipole moments directed from the metal to the molecule, have negative values for $\Delta\Phi$, which lead to lower work functions for the Au metal (Φ_{Au}) (Fig. 2a). In contrast, Perfluoro-C10-S molecules increase the work function of the Au metal (Φ_{Au}) (Fig. 2b). From the perspective of classical electronics, this potential drop, $\Delta\Phi$ (the change in the work function), between the molecule and the metal can be derived from the Helmholtz equation (Eq. (1)) [4,18],

$$\Delta\Phi = -\frac{N_o\mu_{\perp}}{\epsilon_o K_{\text{SAM}}} = -\frac{N_o\mu}{\epsilon_o K_{\text{SAM}}} \cos\theta \quad (1)$$

where N_o is the grafting density (or the dipole moment density) of the SAM ($\#/m^2$) at room temperature, μ_{\perp} is the effective dipole moment of the SAM along the direction perpendicular to the metal substrate, θ is the tilt angle of the molecules with respect to the surface normal of the metal substrate ($\mu_{\perp} = \mu \cos\theta$), ϵ_o is the permittivity of vacuum, and K_{SAM} is the dielectric constant of the SAM. The grafting density (N_o) of the SAM on the Au surface depends on the type of close-packed structure of the molecules on the Au surface. For Naph-S on an Au(111) surface, the molecular chains are oriented closer to the plane of the Au surface ($\theta = \sim 44^\circ$) and adopt an ordered $3 \times 3\sqrt{3}$ (Wood's notation) structure with a rectangular unit cell because of the contributions from the larger nearest-neighbor spacing and the molecular structure, which yields a less dense packing than that of alkanethiol [4,21]. This results in a grafting density (N_o) for the Naph-S SAM of $\sim 2.9 \times 10^{18} \text{ m}^{-2}$ on the Au(111) surface [21]. It is known that Perfluoro-C10-S on an Au(111) surface adopts an ordered $c(7 \times 7)$ superlattice of closed-packed molecules with a lattice constant of 5.8 ± 0.1 Å and a smaller tilt angle ($12\text{--}20^\circ$) [4,22,23]. From these values, the grafting density for the Perfluoro-C10-S SAM can be estimated to be $\sim 3.4 \times 10^{18} \text{ m}^{-2}$ on Au(111) [4]. For the Naph-NC SAM, the exact values of N and θ are not known. Here, we assume that N and θ for the Naph-NC SAM are the same as those for the Naph-S SAM because the molecular structure is the same although a different chemical anchoring group on Au surface. The physical properties

Table 1

Summary of the properties of SAM on Au. Note that the dielectric constants of Naph-NC and Perfluoro-C10-S are from isocyanide film [27] and from poly(tetrafluoroethylene) (PTFE) [4,25].

	K_{SAM}	N_0 ($\times 10^{18} \text{ m}^{-2}$)	θ ($^\circ$)	μ (D)	$\Delta\Phi_{calc}$ (eV)	$\Delta\Phi_{meas}$ (eV)	$\Delta\Phi_W/\Delta T$ ($\times 10^{-4} \text{ eV K}^{-1}$)
$C_{10}H_7S$ (Naph-S)-Au	2.5	2.9 [21]	44 [21]	1.1	-0.34	-0.28 ± 0.06	23.9 ± 8.69
$C_{10}H_7NC$ (Naph-NC)-Au	3.5 [26]	2.9 [21]	44 [21]	4.6	-1.02	-0.70 ± 0.07	66.5 ± 10.7
$C_{10}H_4F_{17}S$ (Perfluoro-C10-S)-Au	2.1 [4,24]	3.4 [4]	12-20 [4,22,23]	2	1.15	0.88 ± 0.05	40.7 ± 7.09

Table 2

Summary of energy required to desorb one molecule from the SAM on Au.

	$E_{SAM(n)}$ (kcal/mol)	$E_{SAM(n-1)}$ (kcal/mol)	E_{mol} (kcal/mol)	$(E_{SAM(n-1)} + E_{mol}) - E_{SAM(n)}$ (kcal/mol)
$C_{10}H_7S$ (Naph-S)-Au	117	109	22	-14
$C_{10}H_7NC$ (Naph-NC)-Au	69	60	22	-13
$C_{10}H_4F_{17}S$ (Perfluoro-C10-S)-Au	17	34	26	-43

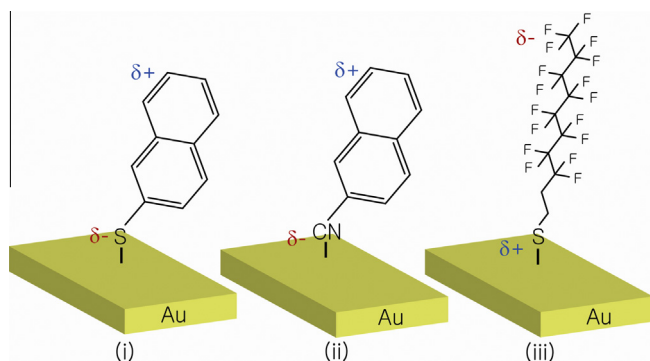


Fig. 1. Schematics of SAM-modified Au metal with (i) Naph-S, (ii) Naph-NC, and (iii) Perfluoro-C10-S. The δ^- and δ^+ depict the negative charge (δ^-) and the positive charge (δ^+), respectively, at the SAM/Au interface.

of the three types of molecules and the calculated and measured interfacial potential drops ($\Delta\Phi_{calc}$ and $\Delta\Phi_{meas}$) on the Au surface are summarized in Table 1.

Fig. 3 shows the work functions for Au (unmodified and modified with SAM) at room temperature; in Fig. 3, the experimental values were measured with a Kelvin probe and the calculated

values were estimated through the Helmholtz equation (Eq. (1)). We measured the work function for the unmodified Au to be $\Phi_{Au} \approx 4.94 \pm 0.06$ eV, whereas SAM of Naph-S, Naph-NC, and Perfluoro-C10-S shifted Φ_W to 4.66 ± 0.12 , 4.24 ± 0.13 , and 5.82 ± 0.11 eV, respectively. The error bars in Fig. 3 represents the standard deviation of the junction ($> \sim 10$ devices for each molecule type). These experimental results were in qualitative agreement with the calculated work functions for the SAM-modified Au estimated with Eq. (1), as summarized in Fig. 3. Furthermore, we found that the work function of the Naph-NC SAM-modified Au metal was smaller than that of the Naph-S SAM-modified Au metal. This result is because the isocyanide anchoring group ($-NC$) has a larger polarity (higher dipole moment) than the thiol group ($-S$), and this larger polarity can lead to a larger potential drop $\Delta\Phi$ at the molecule/Au interface (Table 1).

We characterized the temperature-dependent work functions of the SAM-modified Au to understand the electrical properties of SAM-modified Au if the junction temperature is increased. Fig. 4a shows the change in the work function Φ_W and in the potential drop $\Delta\Phi$ of the SAM-modified Au at different temperatures (300, 323, 343, 363 and 383 K). As the temperature is increased, the work functions of the SAM-modified Au substrates approach the work function of the unmodified Au substrate ~ 4.94 eV (or the potential drop approaches zero, $\Delta\Phi = 0$). At high temperature,

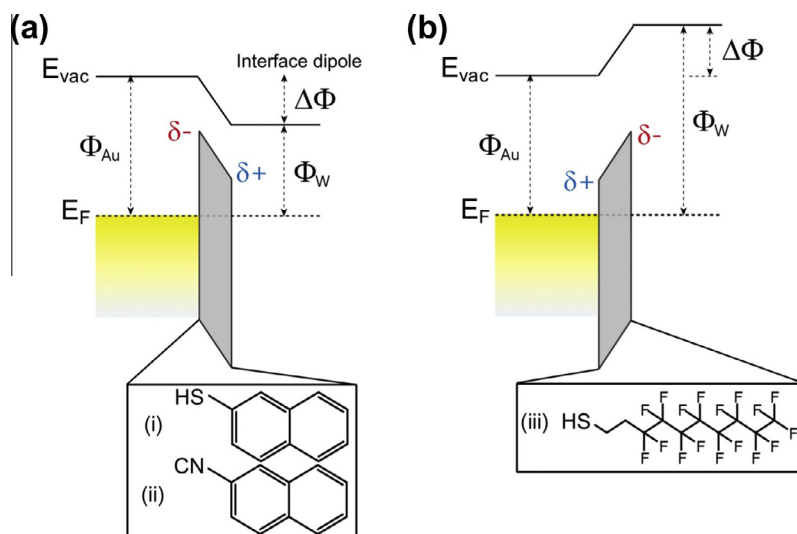


Fig. 2. Schematic energy level diagrams at the SAM/Au interface with an Au work function of Φ_{Au} , a potential drop of $\Delta\Phi$, and a work function of Φ_W for the SAM-modified Au metal. (a) Naph-S and Naph-NC impose an interfacial dipole that lowers $\Delta\Phi$ and Φ_W . (b) Perfluoro-C10-S imposes an interfacial dipole that raises $\Delta\Phi$ and Φ_W . The δ^- and δ^+ depict the direction of the interfacial dipole. E_F is the Fermi level of Au. E_{vac} is the vacuum energy level.

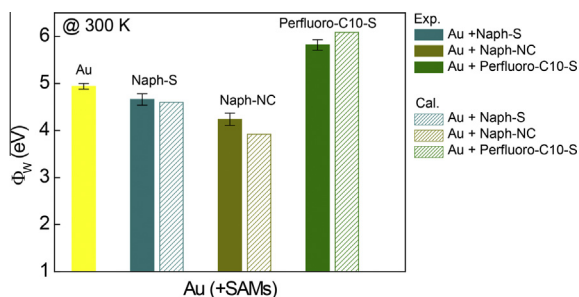


Fig. 3. Work function values for unmodified and SAM-modified Au metal; these values were measured with the Kelvin probe technique and were calculated with the Helmholtz equation (Eq. (1)).

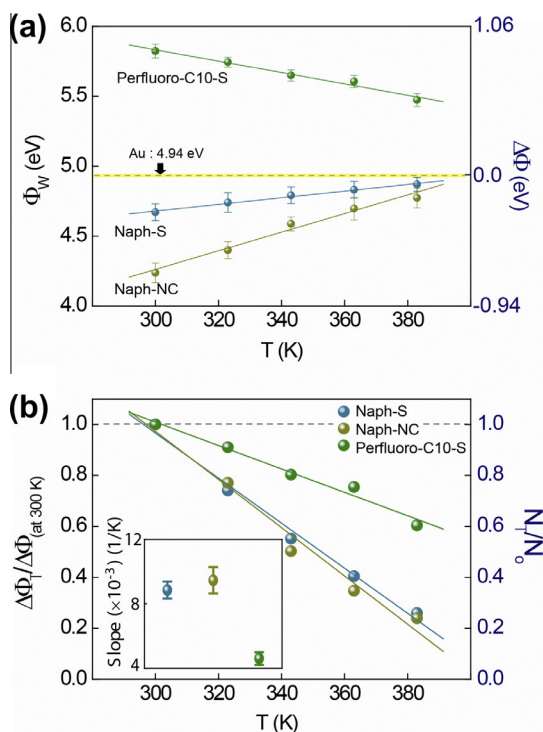


Fig. 4. (a) The work function Φ_w and the potential drop $\Delta\Phi$ for SAM-modified Au metal measured with a Kelvin probe as a function of temperature T . The average work function for unmodified Au metal was $\Phi_{Au} \approx 4.94$ eV (marked with the yellow line). (b) The thermal stability of the SAM-modified Au metal given by the calculated N_T/N_0 values and the experimental $\Delta\Phi_T/\Delta\Phi_{300K}$ values as a function of temperature T . The inset shows the slope of the N_T/N_0 as a function of T for the SAM-modified Au metal. (For interpretation of the references to color in this figure legend, the reader is referred to the web version of this article.)

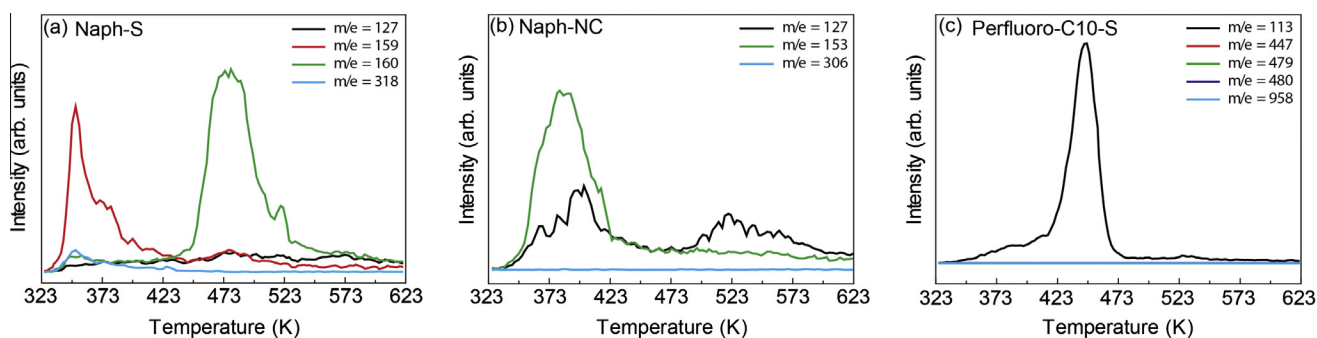


Fig. 5. TD spectra showing the remarkable differences in thermal desorption behaviors of the SAMs of (a) Naph-SH, (b) Naph-NC, and (c) Perfluoro-C10 on Au surfaces.

molecules can be desorbed from the metal surface, and the corresponding molecular configuration can be changed [5,16]; this desorption can lead to a reduction in the potential drop $\Delta\Phi$ at the SAM/metal interface. The slope of $|\Delta\Phi_w/\Delta T|$ in Fig. 4a reflects the reduction in the potential drop $\Delta\Phi$ from molecular desorption as the temperature is increased. We noted that at full coverage (N_0) and room temperature, the molecules are ideally in a “standing phase” configuration with their long axes close to the metal surface normal [4,16]. In contrast, a “lying-down phase” configuration of the molecules was often observed at low coverage or at high temperatures because of the decreased intermolecular van der Waals forces [5,16,27]. In fact, the lying-down phase reduces the potential drop $\Delta\Phi$ at the SAM/Au interface because of the larger molecular tilt angle θ relative to the surface normal of the metal. We can also note that the annealing at high temperature could affect the grain boundaries of Au substrate, which might lead to change the ordering of SAM on Au [16].

The degree of molecular desorption at elevated temperatures can be inferred from the relation between the grafting density N_0 and the potential drop $\Delta\Phi$ in the Helmholtz equation (Eq. (1)). Fig. 4b shows the calculated N_T/N_0 values and the experimental $\Delta\Phi_T/\Delta\Phi_{300K}$ values as a function of temperature for three different types of SAM-modified Au substrates. Here, N_T is the molecular grafting (or dipole moment) density at the temperature T . Similarly, $\Delta\Phi_T$ is the interfacial potential drop at T . The slope of N_T/N_0 as a function of T reflects the decrease in the grafting density of the molecules as the temperature is increased, as shown in the inset in Fig. 4b. A larger slope implies a faster decrease in the grafting density of the molecules on Au metal; in other words, the molecules are easily desorbed from the substrate because of their relative lower binding energies and poorer thermal stabilities. We found that the magnitudes of the slopes were $Naph-NC \geq Naph-S$ (Perfluoro-C10-S) based on the Kelvin probe measurement. This result means that molecules are easily desorbed in the same order; Naph-NC is easier than Naph-S, which is easier than Perfluoro-C10-S. Therefore, the magnitudes of the molecular binding energies are simply expected to be in the opposite order of the desorption rates; that is, Perfluoro-C10-S > Naph-S \geq Naph-NC.

TDS measurements were performed to examine and compare the thermal stabilities and desorption behaviors of SAM on Au surfaces. Fig. 5 shows a clear difference in the thermal desorption behavior and the stability of these SAMs. Especially, the thermal desorption processes of the SAMs containing the naphthalene moiety (Fig. 5a and b) are different from that of the SAM containing the fluorinated alkyl chain moiety (Fig. 5c). Both SAMs of Naph-S and Naph-NC have strong desorption peaks of the parent molecular species ($m/e = 160$ for Naph-SH+ and $m/e = 153$ for Naph-NC+), whereas the Perfluoro-C10-S SAMs has no such parent desorption peak ($m/e = 480$). These desorption behaviors are consistent with the observed change of the work function for these SAMs (Fig. 4).

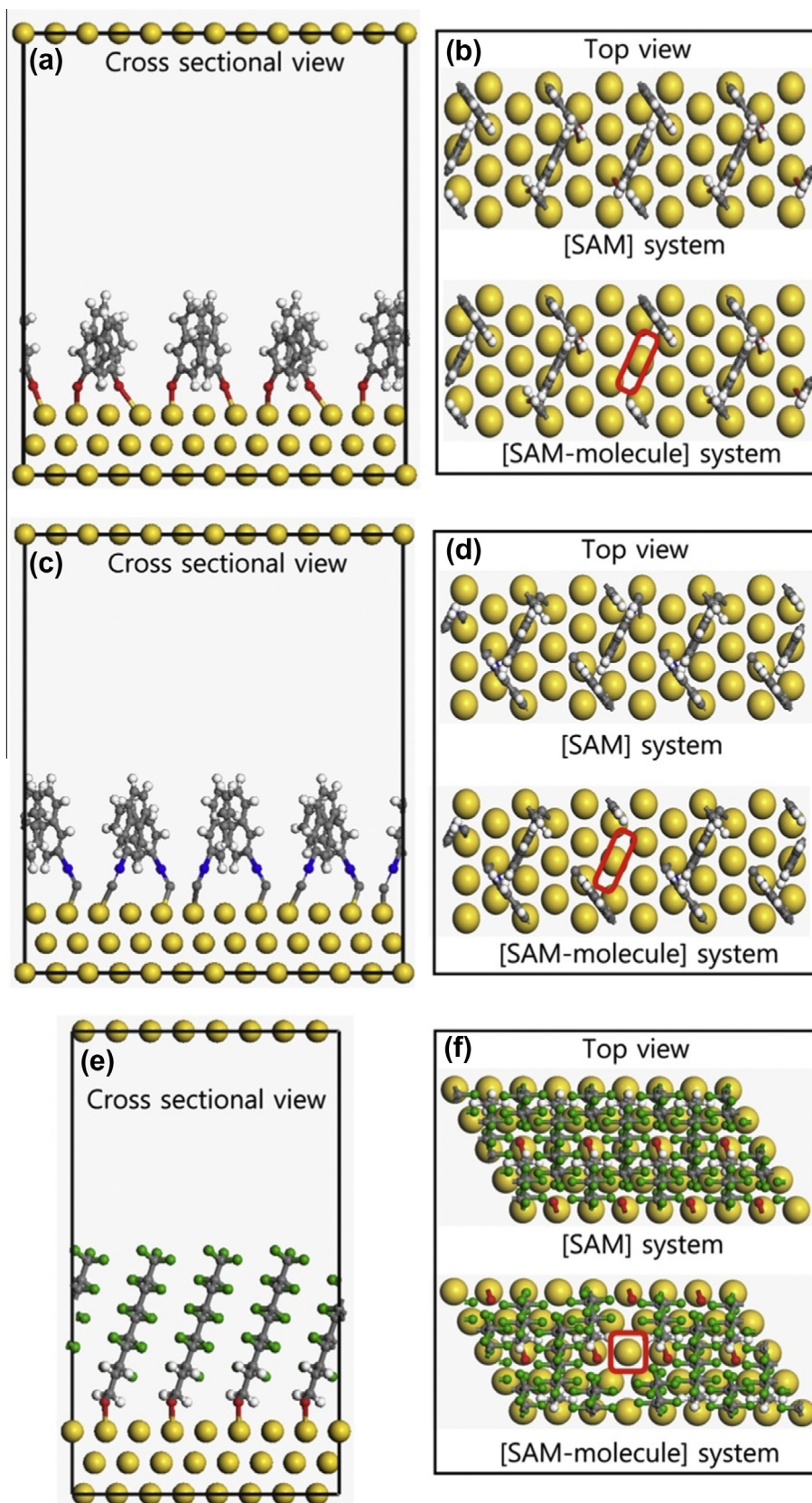


Fig. 6. The cross-sectional and top views of each structural model for Naph-S (a and b), Naph-NC (c and d), and Perfluoro-C10-S (e and f) SAM on Au. In these models, the $(3 \times 3\sqrt{3})$ structure for Naph-S and Naph-NC and the $c(7 \times 7)$ structure for Perfluoro-C10-S are constructed identically to previous experiments [4,21–23]. The vacuum gap between the topmost molecular atom and the next slab was 30 Å. Note that the red boxes in (b), (d), and (f) indicate vacancies from desorbed molecules in the SAM system.

As the Naph-S- and Naph-NC-modified SAMs showed nearly similar slopes in the change of the work function, the Perfluoro-C10-S-modified SAM showed quite different slope (Fig. 4b). For the Naph-S-modified SAMs on Au, two main desorption peaks corresponding to the doubly ionized dimer fragments ($m/e = 159$, Naph-S⁺) and the parent fragments ($m/e = 160$, Naph-SH⁺) were observed at 341 and 473 K, respectively, which might be derived from a hydrogen abstraction reaction of the chemisorbed molecular species from the walls inside the chamber or/and the SAM surface [28–31]. For the Naph-NC-modified SAMs on Au, they show the desorption of the parent molecular species ($m/e = 153$, Naph-NC⁺) in very strong intensity after the cleavage of the C–Au bond at 380 K (Fig. 5b). Although the decomposed fragments ($m/e = 127$, Naph⁺) derived from the cleavage of the C–S bond in the SAMs of Naph-SH were not detectable significantly, we observed relatively strong desorption peak of the decomposed fragments derived from the cleavage of the NaphC–N bond for the SAMs of Naph-NC at 393 and 518 K. We suggest that the advent of the decomposed peak at 518 K may be due to the structural change of the SAMs resulting from the desorption of the adsorbed molecules from the Au surface. Contrary to the SAMs of Naph-S, we did not observe the dimer species [$m/e = 306$, (Naph-NC)₂⁺], which means that the dimerization of the –NC group did not occur during the heating. The thermal desorption behavior of the Perfluoro-C10-modified SAMs on Au was completely different from those of the Naph-S- and Naph-NC-modified SAMs. There were no desorption peaks from the chemisorbed molecular species [$m/e = 479$, perfluorodecanthiolate (R–S⁺)], parent molecular species [$m/e = 480$, perfluorodecanthiolate (R–SH⁺)], dimer [$m/e = 958$, diperfluorodecane disulfide (R–S–S–R⁺)], nor decomposed fragments ($m/e = 447$, R⁺) after the cleavage of the C–S bond (Fig. 5c). These kinds of desorption peaks are usually observed from the n-alkanethiol SAMs on Au. Instead of these peaks, we observed the very strong decomposed fragments ($m/e = 113$) of unknown nature at 450 K. Decomposition of the molecules is initiated slowly from 343 K, and decomposition intensity steeply increased above 415 K, which is consistent with the recent X-ray photoelectron spectroscopy (XPS) results showing the sudden decrease in the fluorine intensity above 423 K [32].

From this all observation, we confirmed that Perfluoro-C10-S-modified SAM on Au had higher thermal stability than the Naph-S- and Naph-NC-modified SAM; this finding is consistent with the observed tendency for the work function changes, which implies that the thermal desorption behaviors and thermal stabilities of the SAM are strongly influenced by the anchoring headgroup and molecular backbone structures.

In order to estimate the molecular binding energy, we used the classical molecular mechanics calculation. The Au(111) surface was represented by a periodic, three-layer slab, and the SAM of each molecule was prepared with the adsorption geometry and packing density proposed from experiments [4,21,22], as shown in Fig. 6. The binding energy corresponds to the desorption energy required to remove one molecule from the SAMs (composed of n molecules) into the gas phase (leaving behind a SAM composed of $n - 1$ molecules); that is, binding energy = $(E_{\text{SAM}(n-1)} + E_{\text{mol}}) - E_{\text{SAM}(n)}$. Here, $E_{\text{SAM}(n)}$ and $E_{\text{SAM}(n-1)}$ are the energy of the SAM consisting of n and $n - 1$ molecules adsorbed on Au(111), respectively. Additionally, E_{mol} is the energy of an isolated molecule in the gas phase. For each species (Naph-S, Naph-NC, and Perfluoro-C10-S), these energy values were calculated in the final geometries, which were optimized with the conjugate gradient method for the universal force field (UFF) [19,20] implemented in Forcite (Accelrys). From this molecular mechanics calculations, we found that Perfluoro-C10-S binds the most strongly (with a binding energy of ~43 kcal/mol) of the three species and is followed by Naph-S (~14 kcal/mol) and Naph-NC (~13 kcal/mol) (see Table 2), which is also consistent with our experimental results (Figs. 4 and 5).

4. Conclusions

We investigated the work function of SAM-modified Au metal at the annealed temperatures. The work function of SAM-modified Au metal approached the work function of the unmodified Au regardless of the direction or magnitude of the dipole moment of the SAM species as the temperature was increased. These observations can be explained by the degree of thermal desorption of the molecular dipole layers. From thermal desorption spectroscopic measurements and molecular modeling calculations, we demonstrated that the thermal molecular desorption and the thermal stability of the SAM on the metal were strongly influenced by the molecular binding energy that depended on the anchoring headgroup and molecular backbone structures. This study extends our understandings of the influences of molecular desorption and binding energy at the SAM/electrode interfaces on the electronic properties of organic-based devices if the devices are treated by thermal annealing to improve device performance. Furthermore, the control of the work function of SAM-modified electrode by thermal annealing will allow the fine tuning of the electrical properties of organic-based devices.

Acknowledgments

The authors thank the National Creative Research Laboratory program (Grant No. 2012026372), the National Core Research Center (Grant No. R15-2008-006-03002-0), and the Basic Science Research Program (2012R1A6A3A03037713) through the National Research Foundation (NRF) of Korea. We specially thank to Dr. James M Tour for the discussion on our manuscript.

References

- [1] I.H. Campbell, J.D. Kress, R.L. Martin, D.L. Smith, N.N. Barashkov, J.P. Ferraris, *Appl. Phys. Lett.* 71 (1997) 3528.
- [2] E.L. Bruner, N. Koch, A.R. Span, S.L. Bernasek, A. Kahn, J. Schwartz, *J. Am. Chem. Soc.* 124 (2002) 3192.
- [3] H. Yan, Q. Huang, J. Cui, J.G.C. Veinot, M.M. Kern, T.J. Marks, *Adv. Mater.* 15 (2003) 835.
- [4] B. de Boer, A. Hadipour, M.M. Mandoc, T. van Woudenberg, P.W.M. Blom, *Adv. Mater.* 17 (2005) 621.
- [5] K. Asadi, F. Gholamrezaie, E.C.P. Smits, P.W.M. Blom, B. de Boer, *J. Mater. Chem.* 17 (2007) 1947–1953.
- [6] P.C. Rusu, G. Giovannetti, G. Brocks, *J. Phys. Chem. C* 111 (2007) 14448.
- [7] F. Rissner, G.M. Rangger, O.T. Hofmann, A.M. Track, G. Heimel, E. Zojer, *ACS Nano* 3 (2009) 3513.
- [8] L. Miozzo, A. Yassar, G. Horowitz, *J. Mater. Chem.* 20 (2010) 2513.
- [9] D. Boudinet, M. Benwadih, Y. Qi, S. Altazin, J.-M. Verilhac, M. Kroger, C. Serbutoviez, R. Gwoziecki, R. Coppard, G. Le Blevenec, A. Kahn, G. Horowitz, *Org. Electron.* 11 (2010) 227.
- [10] J. Niederhausen, P. Amsalem, J. Frisch, A. Wilke, A. Vollmer, R. Rieger, K. Müllen, J.P. Rabe, N. Koch, *Phys. Rev. B* 84 (2011) 165302.
- [11] D. Otálvaro, T. Veening, G. Brocks, *J. Phys. Chem. C* 116 (2012) 7826.
- [12] G. Heimel, L. Romaner, J.-L. Brédas, E. Zojer, *Phys. Rev. Lett.* 96 (2006) 196806.
- [13] B.H. Hamadani, D.A. Corley, J.W. Ciszek, J.M. Tour, D. Natelson, *Nano Lett.* 6 (2006) 1303.
- [14] F. Gholamrezaie, S.G.J. Mathijssen, E.C.P. Smits, T.C.T. Geuns, P.A. van Hal, S.A. Ponomarenko, H.-G. Flesch, R. Resel, E. Cantatore, P.W.M. Blom, D.M. de Leeuw, *Nano Lett.* 10 (2010) 1998.
- [15] H.-G. Flesch, S.G.J. Mathijssen, F. Gholamrezaie, A. Moser, A. Neuhold, J. Novák, S.A. Ponomarenko, Q. Shen, C. Teichert, G. Hlawacek, P. Puschign, C. Ambrosch-Draxl, R. Resel, D.M. de Leeuw, *J. Phys. Chem. C* 115 (2011) 22925.
- [16] Y. Qian, G. Yang, J. Yu, T.A. Jung, G.-Y. Liu, *Langmuir* 19 (2003) 6056.
- [17] P. Fenter, P. Eisenberger, K.S. Liang, *Phys. Rev. Lett.* 70 (1993) 2447.
- [18] N. Peor, R. Sfez, S. Yitzchaik, *J. Am. Chem. Soc.* 130 (2008) 4158.
- [19] A.K. Rappe, C.J. Casewit, K.S. Colwell, W.A. Goddard, W.M. Skiff, *J. Am. Chem. Soc.* 114 (1992) 10024.
- [20] S. Alkis, C. Cao, H.-P. Cheng, J.L. Krause, *J. Phys. Chem. C* 113 (2009) 6360.
- [21] P. Jiang, A. Nion, A. Marchenko, L. Piot, D. Fichou, *J. Am. Chem. Soc.* 128 (2006) 12390.
- [22] K. Tamada, T. Ishida, W. Knoll, H. Fukushima, R. Colorado, M. Graupe, O.E. Shmakova, T.R. Lee, *Langmuir* 17 (2001) 1913.
- [23] G.-Y. Liu, P. Fenter, C.E.D. Chidsey, D.F. Ogletree, P. Eisenberger, M. Salmeron, *J. Chem. Phys.* 101 (1994) 4301.
- [24] D.R. Lede, *Handbook of Chemistry and Physics*, 75th ed., CRC Press, Boca Taton, FL, USA, 1995.

- [25] R.K. Pandeya, K.A. Suresha, V. Lakshminarayanan, J. Colloid Interf. Sci. 315 (2007) 528.
- [26] J. Chen, Molecular Wires, Switches and Memories, Thesis for the Degree of Doctor of Philosophy, Yale University, 2000.
- [27] H.B. Akkerman, A.J. Kronemeijer, P.A. van Hal, D.M. de Leeuw, P.W.M. Blom, B. de Boer, Small 4 (2008) 100.
- [28] J.-L. Lin, B.E. Bent, J. Am. Chem. Soc. 115 (1993) 2849.
- [29] K. Kondoh, C. Kodama, H. Nozoye, J. Phys. Chem. B 102 (1998) 2310.
- [30] E. Ito, H. Ito, H. Kang, T. Hayashi, M. Hara, J. Noh, J. Phys. Chem. C 116 (2012) 17586.
- [31] J. Noh, E. Ito, M.J. Hara, J. Colloid Interf. Sci. 342 (2010) 513.
- [32] A.C. Chandekar, S.K. Sengupta, J.E. Whitten, Appl. Surf. Sci. 256 (2010) 2742.